

**Supporting Information**

**Iron–cobalt–nickel trimetal phosphides embedded onto nitrogen-doped carbon  
materials for overall water splitting**

Jianrui Sun,<sup>a</sup> Saisai Li,<sup>a</sup> Qiaoqiao Zhang,<sup>b</sup> and Jingqi Guan<sup>\*b</sup>

<sup>a</sup> School of Chemistry and Life Science, Changchun University of Technology,  
Changchun 130012, Jilin, China.

<sup>b</sup> Key Laboratory of Surface and Interface Chemistry of Jilin Province, College of  
Chemistry, Jilin University, Changchun 130021, PR China.

\*E-mail: guanjq@jlu.edu.cn (J. Guan)

## **Material characterizations**

Powder X-ray diffraction (XRD) patterns were collected using a Shimadzu XRD-6000 with CuK $\alpha$  radiation (40 kV, 30 mA). Raman spectra were recorded on a Raman spectrometer (Renishaw, Inc.) using a 532 nm laser source. The structures of the samples were determined by transmission electron microscopy (TEM) images collected on a HITACHI H-8100 electron microscopy (Hitachi, Tokyo, Japan) operated at 200 kV. The composition of the samples was characterized by energy-dispersive X-ray spectroscopy (EDX) attached to the STEM. The valence state of manganese was determined using XPS recorded on a Thermo ESCALAB 250Xi. The X-ray source selected was monochromatized Al K $\alpha$  source (15 kV, 10.8 mA). Region scans were collected using a 20 eV pass energy. Peak positions were calibrated relative to C 1s peak position at 284.6 eV.

## **Electrochemical activity characterizations**

All electrochemical measurements were performed in a three-electrode system with a glassy carbon electrode (GCE) as the substrate for the working electrode, a graphite rod as the counter electrode and a saturated calomel electrode as the reference electrode. The reference electrode was calibrated with respect to a reversible hydrogen electrode before each experiment. The glassy carbon electrode was pre-polished using 0.05  $\mu$ m alumina and distilled water. To prepare the working electrode, 2 mg of the catalyst was dispersed in a 0.5 mL mixed solvent of ethanol and Nafion (0.25 wt%) and sonicated to obtain a homogeneous ink. A certain amount of the

catalyst ink was drop-casted on the glassy carbon electrode and dried at room temperature.

For OER, the working electrode was first activated by steady-state cyclic voltammetry (CV) performed in the potential range from 1.0 to 1.6 V vs RHE at a scan rate of 50 mV s<sup>-1</sup> for 50 cycles. Linear scan voltammetry (LSV) curves were then collected at a scan rate of 5 mV s<sup>-1</sup>. All of the potentials in the LSV polarization curves were with 90% *iR* compensation unless specifically illustrated.

### **Calibration of SCE and conversion to RHE**

The reference electrode SCE was calibrated according to the method reported previously.<sup>1-3</sup> Calibrations were carried out by using a reversible hydrogen electrode (RHE). First, two Pt electrodes were cleaned by cycling in 1 M H<sub>2</sub>SO<sub>4</sub> between -2 and 2 V for 2 hours. Then, they were used as working electrode and counter electrode, respectively. Before the calibration, the electrolytes 0.1 M KOH and 0.5 M H<sub>2</sub>SO<sub>4</sub> should be saturated with H<sub>2</sub> by continuous bubbling H<sub>2</sub>. During the calibration, hydrogen was bubbled over the working electrode. A series of controlled-potential chronoamperometric curves were measured for 300 s to get the current interconvert between the hydrogen oxidation and hydrogen evolution reaction. The resulting potential is the potential of zero net current. In this work, the potential of zero net current was found at -1.038 V versus the SCE electrode in 1.0 M KOH, and -0.253 V versus the SCE electrode in 0.5 M H<sub>2</sub>SO<sub>4</sub>. Thus, the potentials, measured against SCE, were converted into the potentials versus RHE by using the equations 1-2:

$$\text{In 1.0 M KOH: } E_{\text{vs.RHE}} = E_{\text{vs.SCE}} + 1.038 \text{ V} \quad (1)$$

$$\text{In 0.5 M H}_2\text{SO}_4: E_{\text{vs.RHE}} = E_{\text{vs.SCE}} + 0.253 \text{ V} \quad (2)$$

### **Electrochemically active surface area (ECSA)**

To determine the effective electrochemical active surface area (ECSA) of samples, a series of cyclic voltammetry (CV) curves were tested at various scan rates (10, 20, 40, 60, 80 and 100 mV/s) in the potential window between 0.253 and 0.353 V vs. RHE. The sweep segments of the measurements were set to 10 to ensure consistency. The geometric double layer capacitance ( $C_{dl}$ ) was calculated by plotting the difference of current density  $\Delta J = (J_{anodic} - J_{cathodic})/2$  at 0.303 V vs. RHE against the scan rate, and the slope of the linear trend was  $C_{dl}$ . Finally, the ECSA of catalyst on GCE is estimated according to the equation 3:

$$ECSA = \frac{C_{dl}}{C_s} \quad (3)$$

where  $C_s$  is the specific capacitance of a flat standard electrode with 1 cm<sup>2</sup> of real surface area, which is generally in the range of 20 to 60  $\mu\text{F cm}^{-2}$ .<sup>4,5</sup> In this work, the averaged value of 40  $\mu\text{F cm}^{-2}$  was adopted for the flat electrode.

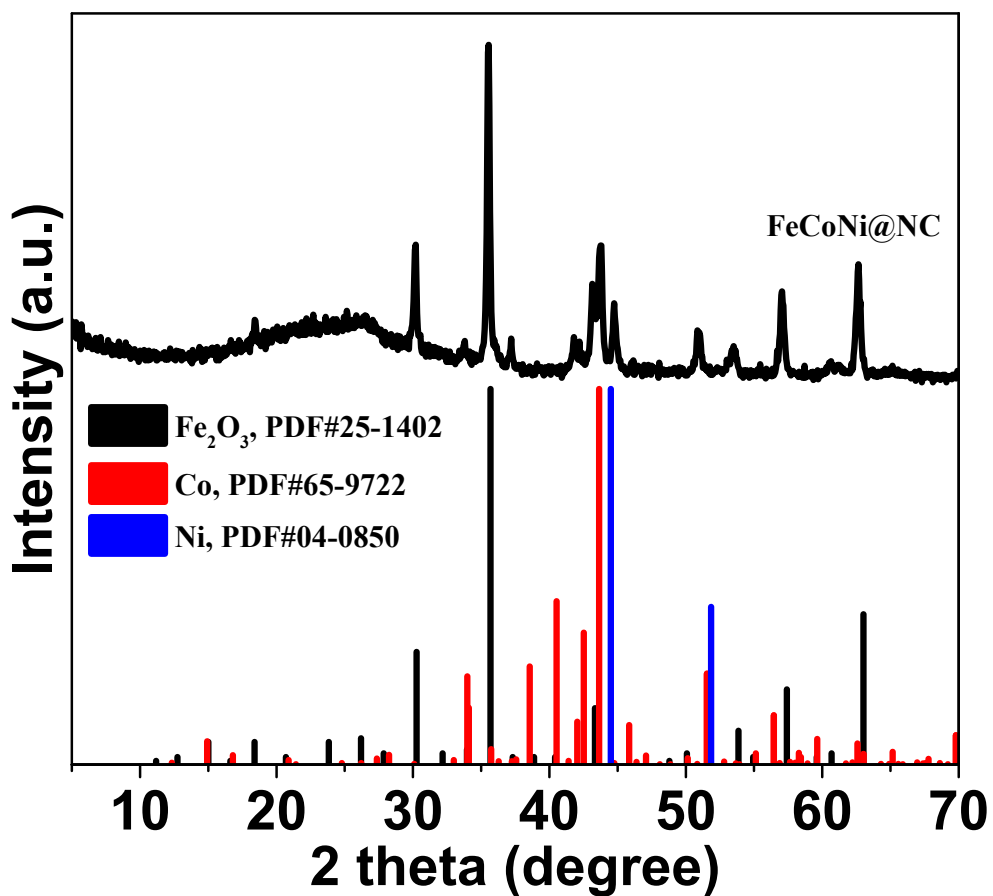


**Figure S1.** XRD patterns of FeCoNi@NC and referred samples.

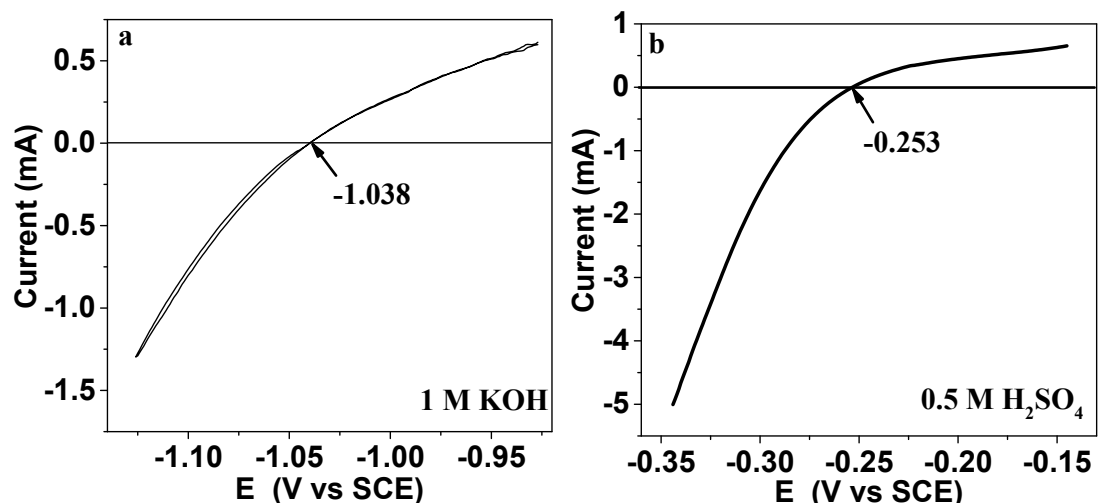


**Figure S2.** The current as a function of the applied potentials for the calibration of SCE reference electrode in 1.0 M KOH (a) and 0.5 M H<sub>2</sub>SO<sub>4</sub> (b).

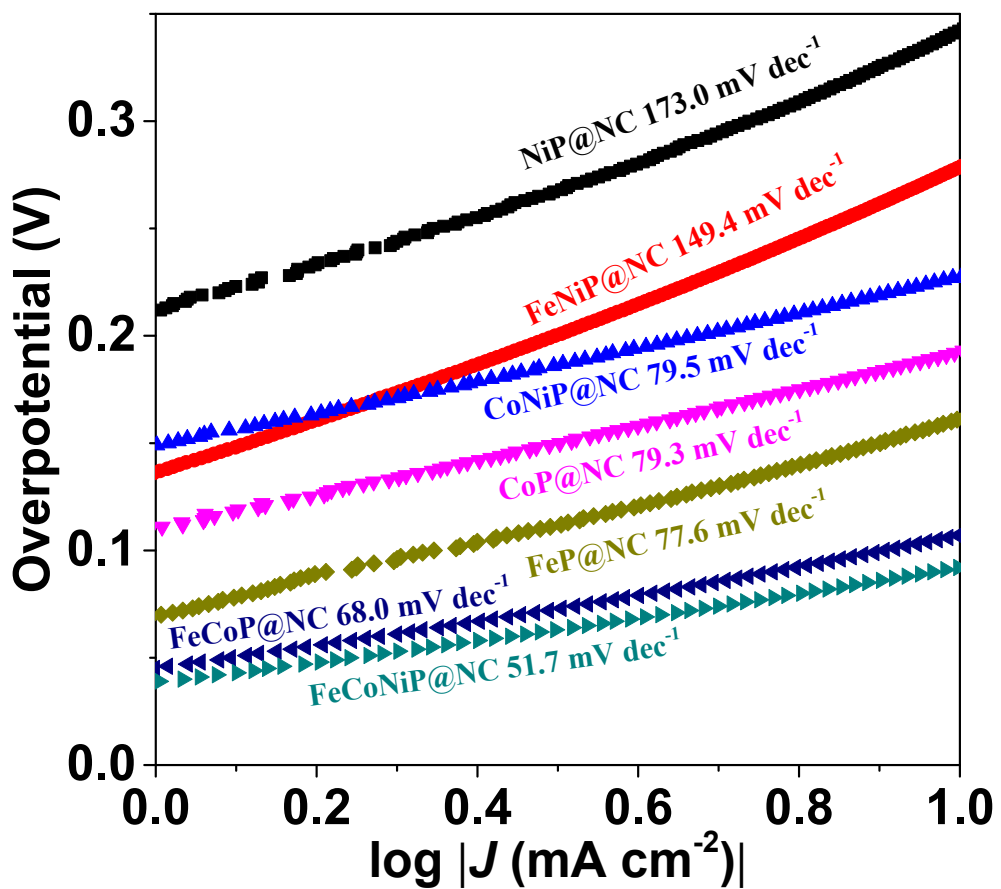


**Figure S3.** Tafel plots for FeP@NC, CoP@NC, NiP@NC, FeCoP@NC, FeNiP@NC, CoNiP@NC, and FeCoNiP@NC in 0.5 M H<sub>2</sub>SO<sub>4</sub>.

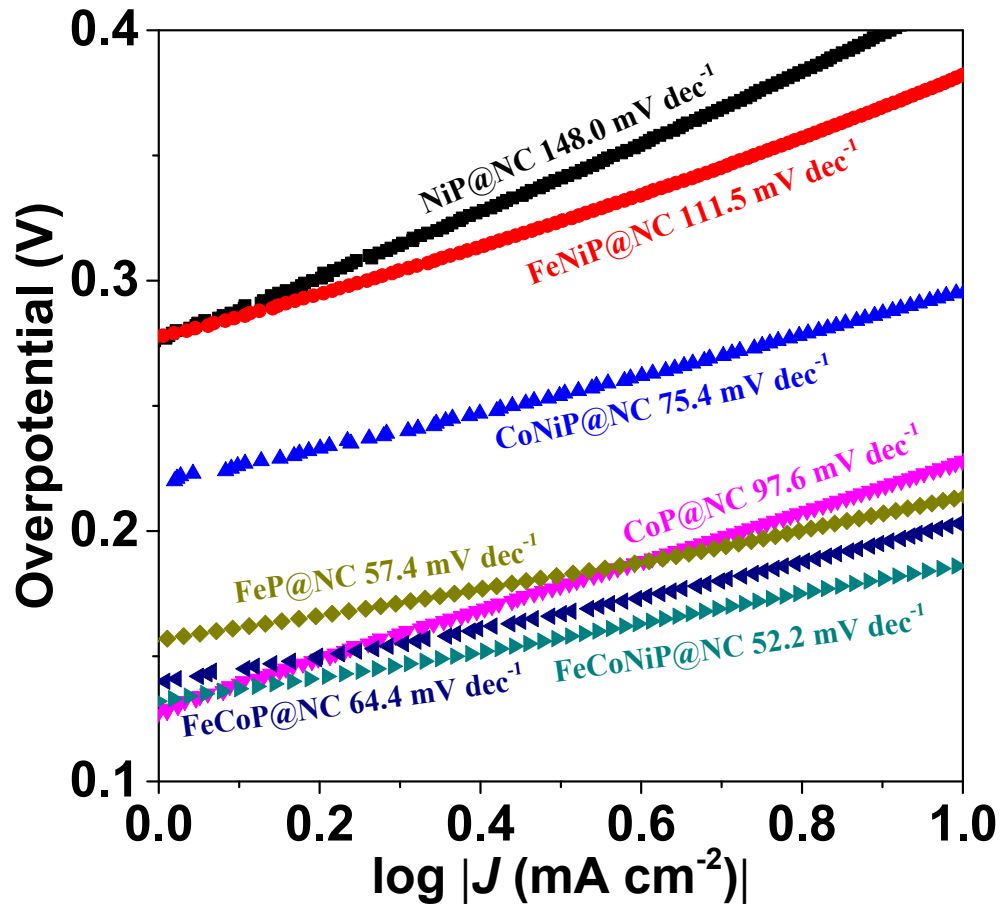


**Figure S4.** Tafel plots for FeP@NC, CoP@NC, NiP@NC, FeCoP@NC, FeNiP@NC, CoNiP@NC, and FeCoNiP@NC in 1.0 M KOH.

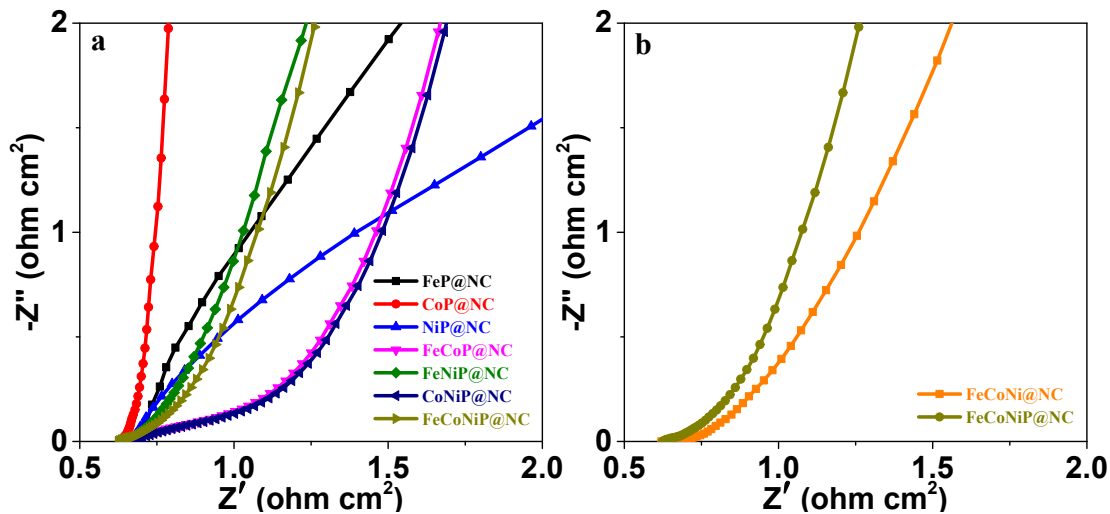


**Figure S5.** (a) Nyquist plots of the EIS test for the FeP@NC, CoP@NC, NiP@NC, FeCoP@NC, FeNiP@NC, CoNiP@NC, and FeCoNiP@NC. (b) Nyquist plots of the EIS test for the FeCoNi@NC and FeCoNiP@NC. The solid lines are the fits to the data using the simplified Randles circuit shown in the inset.

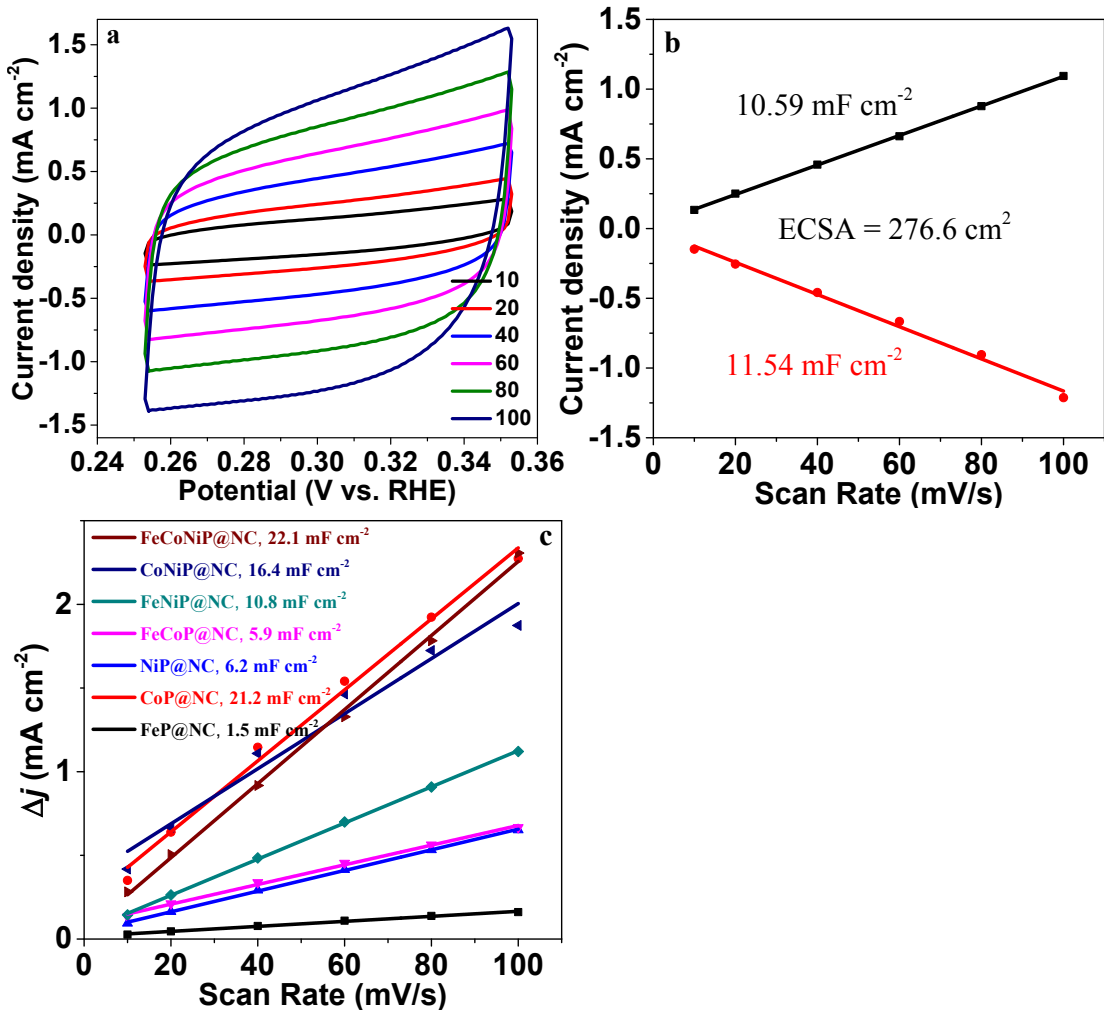


**Figure S6.** (a) CVs of FeCoNiP@NC measured in a non-Faradaic region (from 0 to 0.1 V vs. SCE) at scan rate of 10 mV s<sup>-1</sup>, 20 mV s<sup>-1</sup>, 40 mV s<sup>-1</sup>, 60 mV s<sup>-1</sup>, 80 mV s<sup>-1</sup>, and 100 mV s<sup>-1</sup>. (b) Capacitive  $j$  vs scan rate for FeCoNiP@NC anode. The linear slope is equivalent to twice of the double-layer capacitance  $C_{dl}$ . (c) Capacitive  $j$  vs scan rate for FeP@NC, CoP@NC, NiP@NC, FeCoP@NC, FeNiP@NC, CoNiP@NC, and FeCoNiP@NC.

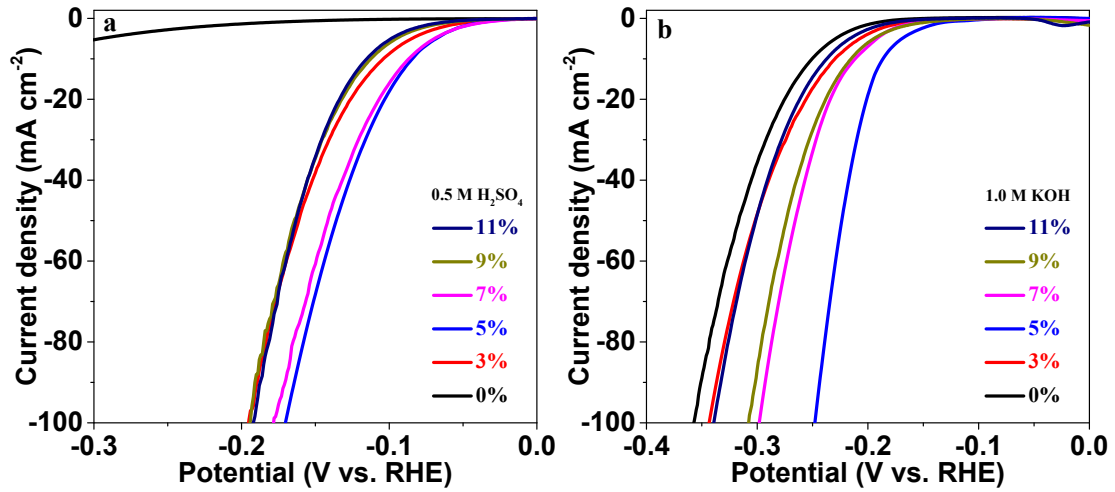


**Figure S7.** Effect of initial graphene oxide content on the HER performance of FeCoNiP@NC in  $0.5 \text{ M H}_2\text{SO}_4$  (a) and  $1.0 \text{ M KOH}$  (b).

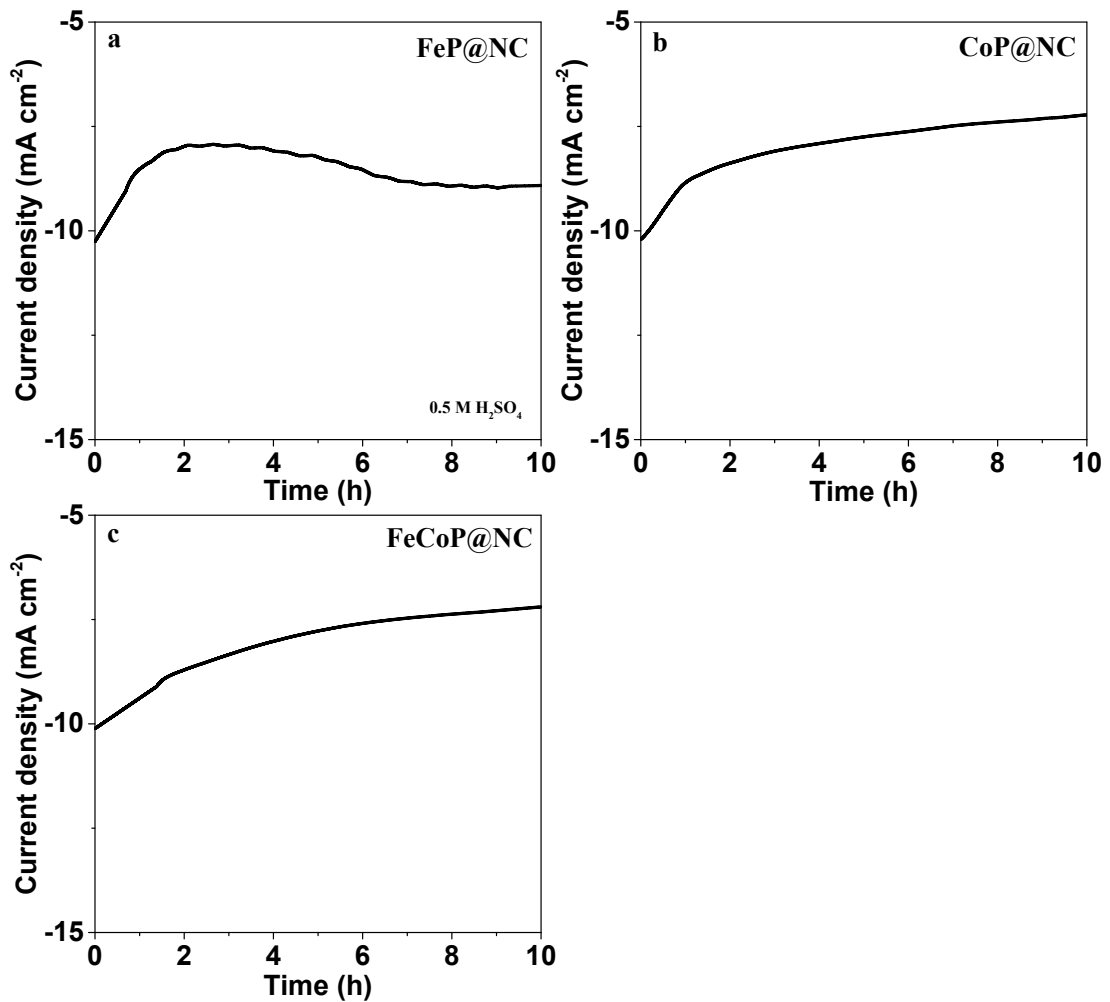


**Figure S8.** Plots of current density vs time for the FeP@NC, CoP@NC, and FeCoP@NC in 0.5 M  $\text{H}_2\text{SO}_4$ .

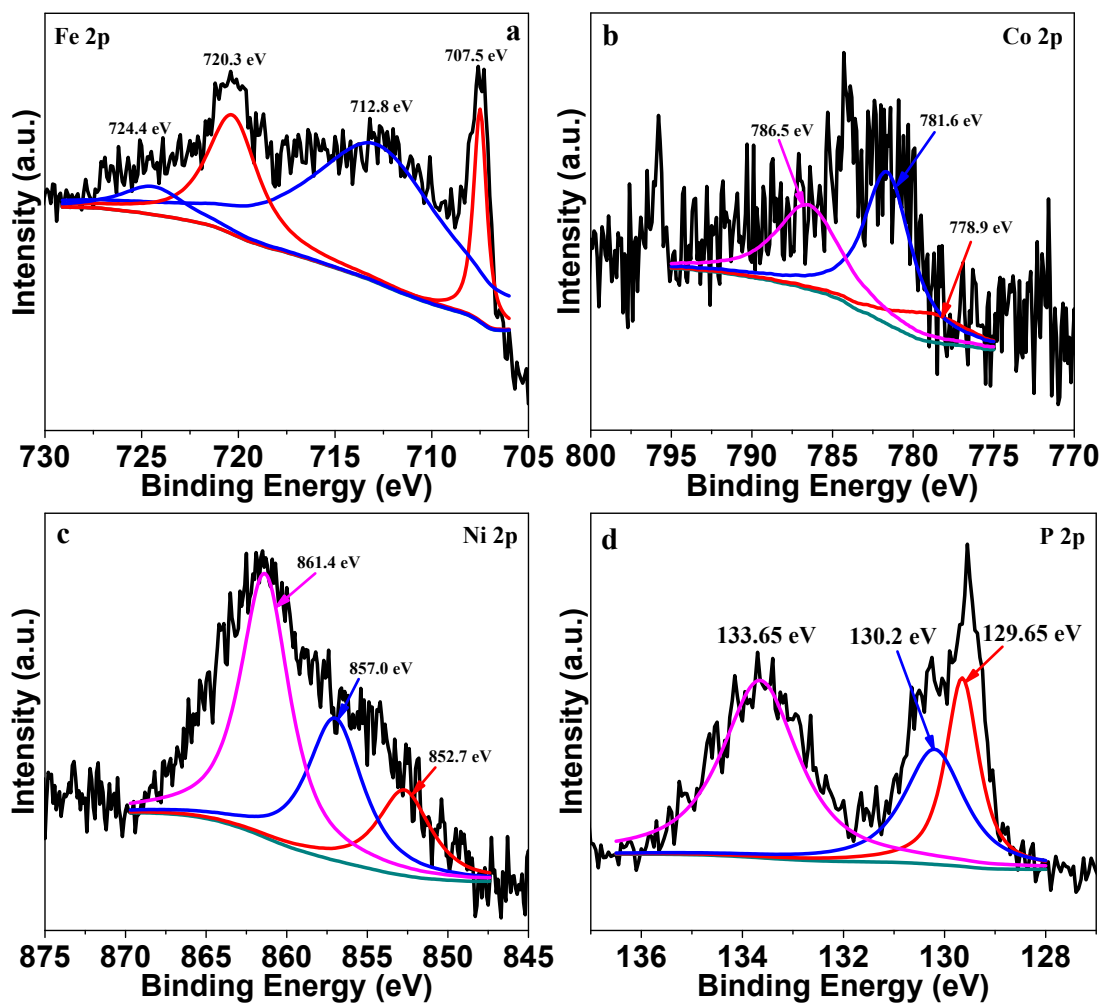


**Figure S9.** The high-resolution Fe2p, Co2p, Ni2p, and P2p XPS spectra of the used FeCoNiP@NC catalyst after HER stability test.

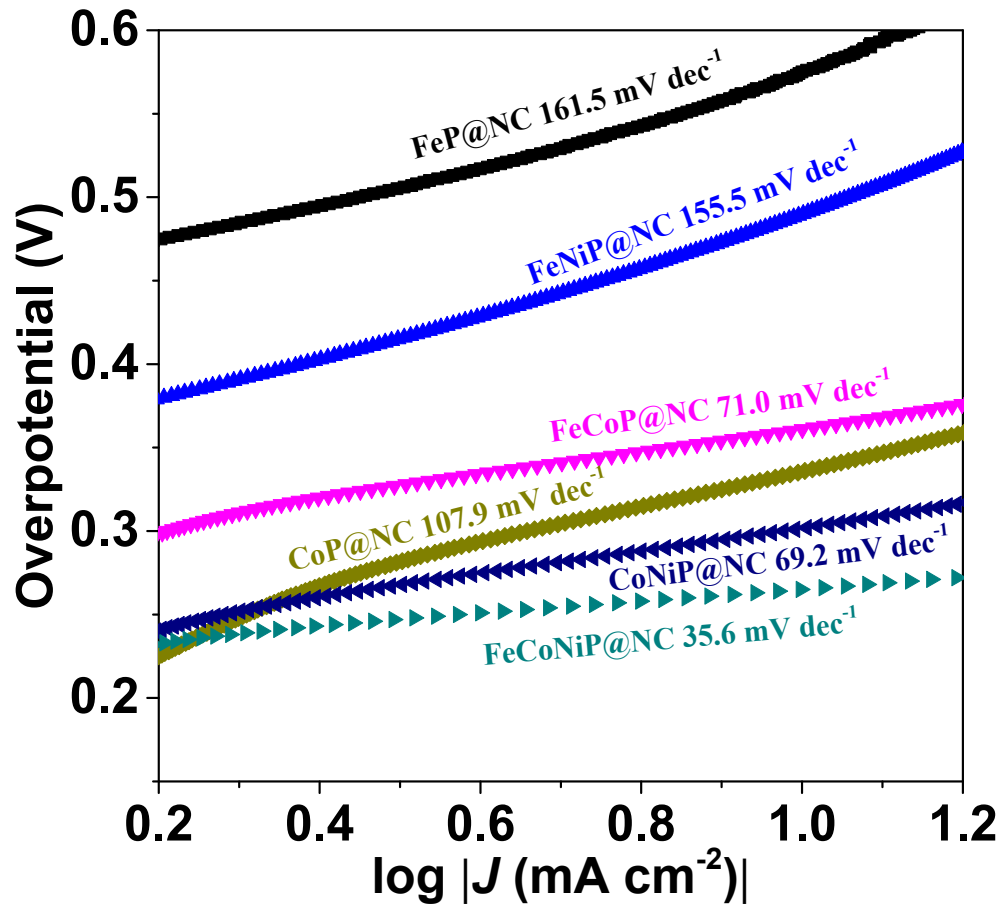


**Figure S10.** Tafel plots for FeP@NC, CoP@NC, FeCoP@NC, FeNiP@NC, CoNiP@NC, and FeCoNiP@NC in 1.0 M KOH.

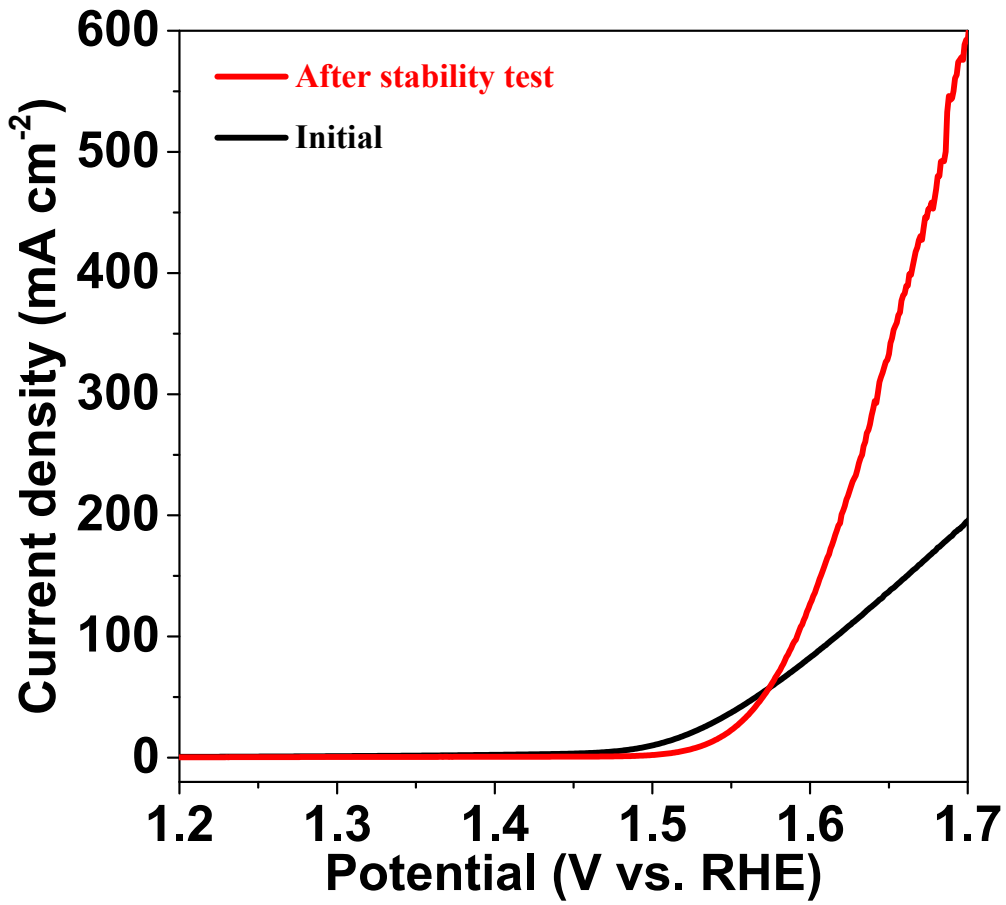


**Figure S11.** LSV curves of FeCoNiP@NC before and after OER stability test in 1.0 M KOH.

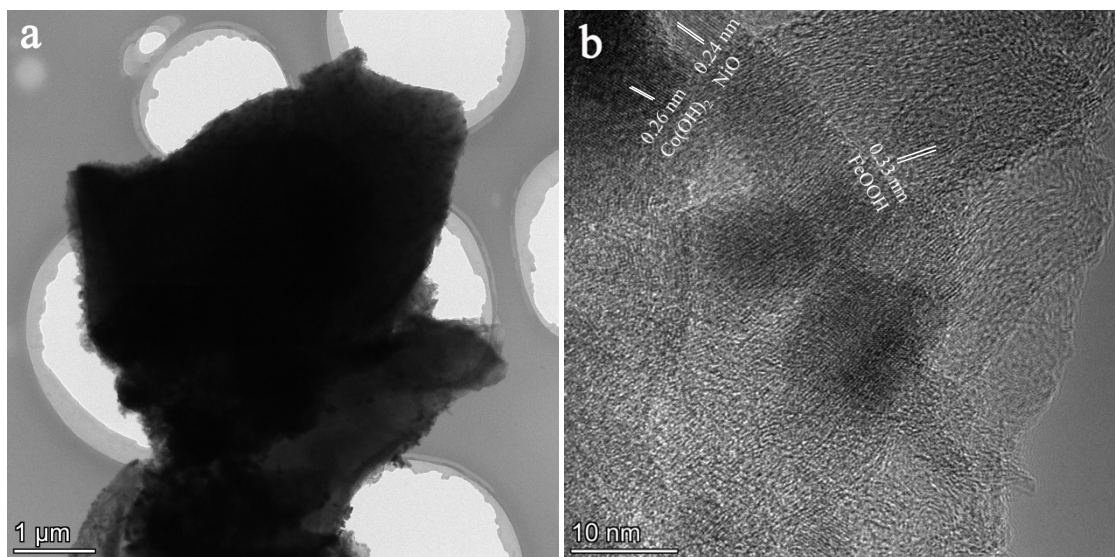


**Figure S12.** (a-b) HRTEM images of FeCoNiP@NC after OER stability test.

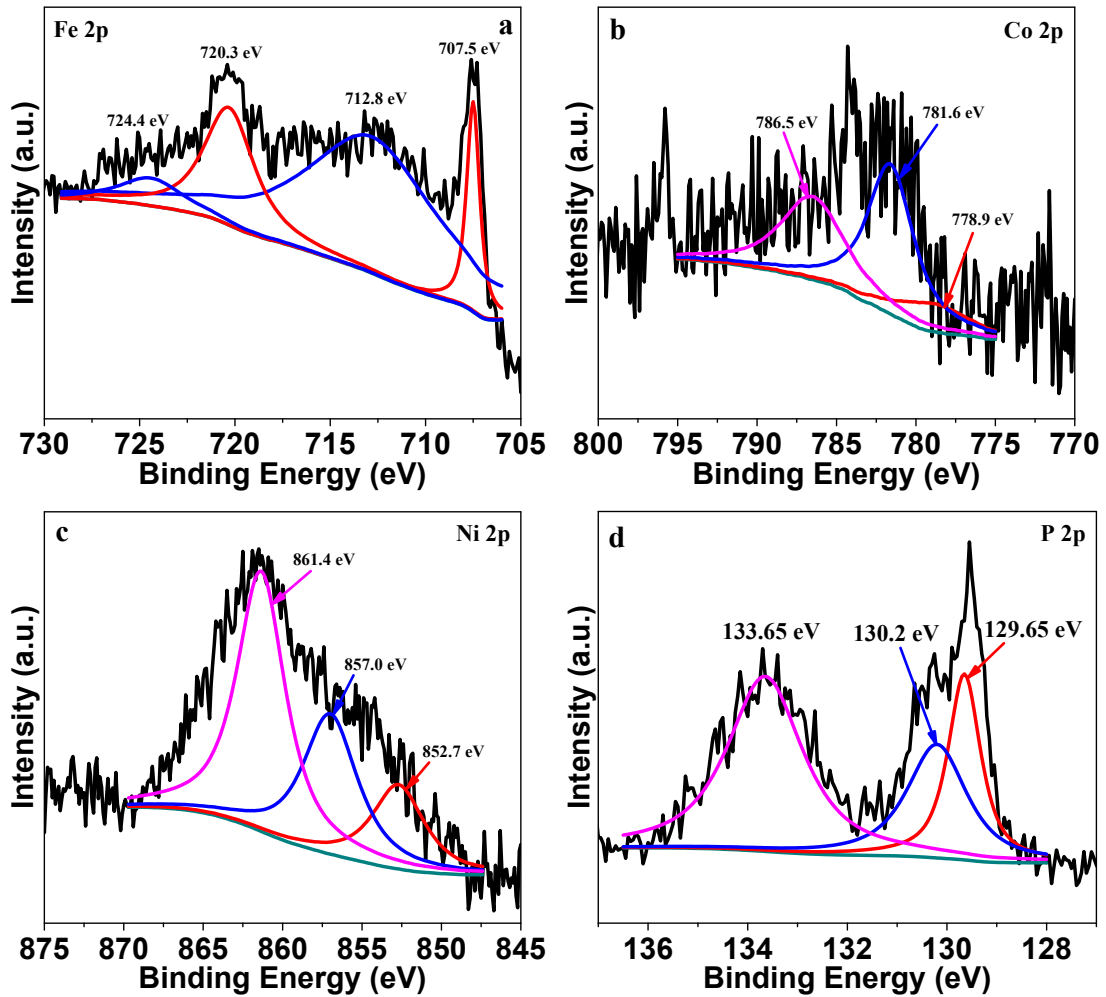


**Figure S13.** High-resolution XPS spectra of Fe 2p (a), Co 2p (b), Ni 2p (c), and P 2p (d) for FeCoNiP@NC after OER stability test.

**Table S1.** Comparison of HER performance with results in recent literature

Catalyst	Electrolyte	$\eta @ 10$ mA·cm <sup>-2</sup>	Tafel slope (mV·dec <sup>-1</sup> )	Ref.
FeCoNiP@NC	0.5 M H <sub>2</sub> SO <sub>4</sub>	93	51.7	This work
FeCoNiP@NC	1.0 M KOH	187	52.2	This work
Porous Co <sub>2</sub> P	0.5 M H <sub>2</sub> SO <sub>4</sub>	150	53	<sup>6</sup>
CoP	0.5 M H <sub>2</sub> SO <sub>4</sub>	170	61	<sup>7</sup>
Co-NG	0.5 M H <sub>2</sub> SO <sub>4</sub>	147	82	<sup>5</sup>
Ni@Ni <sub>2</sub> P–Ru	0.5 M H <sub>2</sub> SO <sub>4</sub>	51	35	<sup>8</sup>
Pt-Ni alloy	0.1 M KOH	65	74	<sup>9</sup>
MoC <sub>x</sub>	1.0 M KOH	151	59	<sup>10</sup>
CoS <sub>2</sub> HNSs	1.0 M KOH	193	100	<sup>11</sup>
Co-NRCNTs	0.5 M H <sub>2</sub> SO <sub>4</sub>	260	69	<sup>12</sup>
CoSe <sub>2</sub> MP/CC	0.5 M H <sub>2</sub> SO <sub>4</sub>	193	50	<sup>13</sup>
Co@NC/NCNS-800	1.0 M KOH	219	55.8	<sup>14</sup>
Co <sub>3</sub> S <sub>4</sub> polyhedra	0.5 M H <sub>2</sub> SO <sub>4</sub>	380	85.3	<sup>15</sup>
Co <sub>0.6</sub> Mo <sub>1.4</sub> N <sub>2</sub>	0.1 M KOH	320	80	<sup>16</sup>
CoP	0.1 M KOH	210	129	<sup>17</sup>
CoMoP NPs	0.5 M H <sub>2</sub> SO <sub>4</sub>	178	60.5	<sup>18</sup>
Co@NiCoP	0.5 M H <sub>2</sub> SO <sub>4</sub>	276	43	<sup>19</sup>

**Table S2.** Comparison of OER performance with results in recent literature

Catalyst	Electrolyte	$\eta @ 10$ mA·cm <sup>-2</sup>	Tafel slope (mV·dec <sup>-1</sup> )	Ref.
FeCoNiP@NC	1.0 M KOH	266	35.6	This work
Ni <sub>2</sub> P	1.0 M KOH	300	64	<sup>20</sup>
Ni <sub>5</sub> P <sub>4</sub>	1.0 M KOH	330	-	<sup>21</sup>
Co <sub>2</sub> P NPs	1.0 M KOH	310	50	<sup>20</sup>
CoP/CC	1.0 M KOH	281	62	<sup>22</sup>
CoP hollow polyhedra	1.0 M KOH	400	57	<sup>23</sup>
CoP MNA	1.0 M KOH	310	65	<sup>24</sup>
CoP/Ti mesh	1.0 M KOH	310	87	
CP@FeP	1.0 M KOH	365	63.6	<sup>25</sup>
FeNi-LDH/CoP	1.0 M KOH	255	33.5	<sup>26</sup>
Co/CoP-5	1.0 M KOH	340	79.5	<sup>27</sup>

## REFERENCES

1. Y. Liang, Y. Li, H. Wang, J. Zhou, J. Wang, T. Regier and H. Dai, *Nat. Mater.*, 2011, **10**, 780-786.
2. Y. Li, W. Zhou, H. Wang, L. Xie, Y. Liang, F. Wei, J.-C. Idrobo, S. J. Pennycook and H. Dai, *Nat. Nanotechnol.*, 2012, **7**, 394-400.
3. M. B. Stevens, L. J. Enman, A. S. Batchellor, M. R. Cosby, A. E. Vise, C. D. M. Trang and S. W. Boettcher, *Chem. Mater.*, 2017, **29**, 120-140.
4. J. Kibsgaard and T. F. Jaramillo, *Angew. Chem., Int. Ed.*, 2014, **53**, 14433-14437.
5. H. Fei, J. Dong, M. J. Arellano-Jimenez, G. Ye, N. D. Kim, E. L. G. Samuel, Z. Peng, Z. Zhu, F. Qin, J. Bao, M. J. Yacaman, P. M. Ajayan, D. Chen and J. M. Tour, *Nat. Commun.*, 2015, **6**, 8668.
6. Y. Yang, H. Fei, G. Ruan and J. M. Tour, *Adv. Mater.*, 2015, **27**, 3175-3180.
7. C. Wang, J. Jiang, X. Zhou, W. Wang, J. Zuo and Q. Yang, *J. Power Sources*, 2015, **286**, 464-469.
8. Y. Liu, S. Liu, Y. Wang, Q. Zhang, L. Gu, S. Zhao, D. Xu, Y. Li, J. Bao and Z. Dai, *J. Am. Chem. Soc.*, 2018, **140**, 2731-2734.
9. Z. Cao, Q. Chen, J. Zhang, H. Li, Y. Jiang, S. Shen, G. Fu, B.-a. Lu, Z. Xie and L. Zheng, *Nat. Commun.*, 2017, **8**, 15131.
10. H. B. Wu, B. Y. Xia, L. Yu, X.-Y. Yu and X. W. Lou, *Nat. Commun.*, 2015, **6**, 6512.
11. X. Ma, W. Zhang, Y. Deng, C. Zhong, W. Hu and X. Han, *Nanoscale*, 2018,

- 10**, 4816-4824.
12. X. Zou, X. Huang, A. Goswami, R. Silva, B. R. Sathe, E. Mikmekova and T. Asefa, *Angew. Chem., Int. Ed.*, 2014, **53**, 4372-4376.
13. Q. Liu, J. Shi, J. Hu, A. M. Asiri, Y. Luo and X. Sun, *ACS Appl. Mater. Interf.*, 2015, **7**, 3877-3881.
14. M. Li, T. Liu, X. Bo, M. Zhou and L. Guo, *J. Mater. Chem. A*, 2017, **5**, 5413-5425.
15. Z.-F. Huang, J. Song, K. Li, M. Tahir, Y.-T. Wang, L. Pan, L. Wang, X. Zhang and J.-J. Zou, *J. Am. Chem. Soc.*, 2016, **138**, 1359-1365.
16. R. Subbaraman, D. Tripkovic, K.-C. Chang, D. Strmenik, A. P. Paulikas, P. Hirunsit, M. Chan, J. Greeley, V. Stamenkovic and N. M. Markovic, *Nat. Mater.*, 2012, **11**, 550-557.
17. J. Tian, Q. Liu, A. M. Asiri and X. Sun, *J. Am. Chem. Soc.*, 2014, **136**, 7587-7590.
18. Y.-Y. Ma, C.-X. Wu, X.-J. Feng, H.-Q. Tan, L.-K. Yan, Y. Liu, Z.-H. Kang, E.-B. Wang and Y.-G. Li, *Energy Environ. Sci.*, 2017, **10**, 788-798.
19. Y. Bai, H. Zhang, L. Liu, H. Xu and Y. Wang, *Chem.-Eur. J.*, 2016, **22**, 1021-1029.
20. S. Anantharaj, S. R. Ede, K. Sakthikumar, K. Karthick, S. Mishra and S. Kundu, *ACS Catal.*, 2016, **6**, 8069-8097.
21. M. Ledendecker, S. Krick Calderón, C. Papp, H. P. Steinrück, M. Antonietti and M. Shalom, *Angew. Chem., Int. Ed.*, 2015, **54**, 12361-12365.

22. P. Wang, F. Song, R. Amal, Y. H. Ng and X. Hu, *ChemSusChem*, 2016, **9**, 472-477.
23. M. Liu and J. Li, *ACS Appl. Mater. Interf.*, 2016, **8**, 2158-2165.
24. Y. P. Zhu, Y. P. Liu, T. Z. Ren and Z. Y. Yuan, *Adv. Funct. Mater.*, 2015, **25**, 7337-7347.
25. D. Xiong, X. Wang, W. Li and L. Liu, *Chem. Commun.*, 2016, **52**, 8711-8714.
26. K. He, T. T. Tsega, X. Liu, J. Zai, X.-H. Li, X. Liu, W. Li, N. Ali and X. Qian, *Angew. Chem., Int. Ed.*, 2019, **58**, 11903-11909.
27. Z.-H. Xue, H. Su, Q.-Y. Yu, B. Zhang, H.-H. Wang, X.-H. Li and J.-S. Chen, *Adv. Energy Mater.*, 2017, **7**, 1602355